

COMPUTATION OF TURBULENT SWIRLING QUARL BURNER FLOW

N. KELSON and D.L S. McELWAIN

Queensland University of Technology, Brisbane, AUSTRALIA

ABSTRACT

A computational study of turbulent flow in a quarl burner is reported. Three eddy viscosity models are used to model the turbulence, two of which include modifications predicted by renormalisation group (RNG) theory. A simple change of model constants to values predicted by the theory yields results which capture the essential flow features. We also demonstrate conclusively that the calculations are extremely sensitive to upstream conditions. Even slightly different inlet profiles which have the same mean flow rate and Swirl number will lead to significant differences in the predictions. For turbulence model assessments in swirling flow, our results underline the need to gauge the sensitivity of computations to any unknown inlet conditions. It is hoped that work described here will motivate experimental studies where upstream conditions are mapped out in even greater detail.

INTRODUCTION

We report here a computational study of vortex breakdown flow in a quarl burner, and results are compared with experimental data from the International Flame Research Foundation (Hagiwara et al., 1986). A schematic of the flow geometry is shown in Fig. 1. The flow in the inlet pipe is close to solid-body rotation, and further downstream a complex two-celled, near-axis inner recirculation zone (IRZ) forms, which is thought to be a manifestation of bubble-type vortex breakdown.

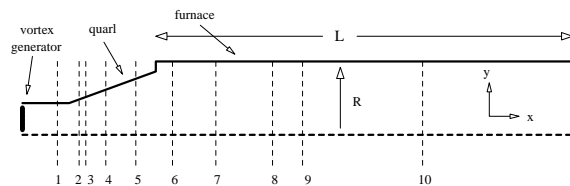


Figure 1: Schematic of flow geometry. Locations of transverse measurement stations are also shown.

An important question is what minimum level of turbulence modelling will be needed to capture the complex features of this recirculating flow. Here we investigate whether eddy viscosity models which include modifications from Renormalisation Group (RNG) theory can successfully model the data set. Although RNG models have been developing for some time, there is still a need for more studies which test these models against available data sets (Smith & Woodruff, 1998). Here, in particular, it is important to gauge the sensitivity of results to the modelled inlet conditions as part of the assessment process, because the upstream concentrated vortex core

flow can act as a fluid amplifier of small changes at the inlet (Hall, 1966). A few computational studies of this flow have been previously reported (Wanik & Schnell, 1989; Benim, 1990; Weber et al., 1990; Orszag et al., 1993). However, the computations of Wanik & Schnell are almost certainly numerically under-resolved, and we believe that the conclusions of Benim's work are also obscured by the use of coarse grid calculations. Orszag et al. gave very few quantitative results, while Weber et al. seem to have used questionable inlet turbulence profiles. For comparison with our results, which differ substantially from previous studies, we shall refer mainly to the works of Benim and Weber et al. in the following.

Turbulence Modelling

In this work we model the turbulence using the standard two-equation k-epsilon model (denoted STD), and RNG modifications to it. In the two-equation modelling approach, the isotropic eddy viscosity is calculated using values of turbulence energy k and dissipation rate ϵ obtained from their respective transport equations. We use the usual values for the empirical constants in STD model: $C_\mu = 0.09, \sigma_k = 1.0, \sigma_\epsilon = 1.3, C_{1\epsilon} = 1.44, C_{2\epsilon} = 1.92$.

In order to gauge the effect of RNG modifications we consider two additional models. In both cases the transport equations are unaltered except for an additional term in the dissipation equation, which may be written in cartesian tensor form as

$$\frac{\partial \epsilon}{\partial t} + \frac{\partial}{\partial x_i} (U_i \epsilon) = \frac{\partial}{\partial x_i} \left(\frac{v_i}{\sigma_\epsilon} \frac{\partial \epsilon}{\partial x_i} \right) + C_{1\epsilon} \frac{\epsilon}{k} v_i S^2 - C_{2\epsilon} \frac{\epsilon^2}{k} - R,$$

where S^2 is the squared magnitude of rate of strain tensor. In the first of the RNG models (denoted R1) we set $R=0$, and change the values of the constants to those predicted by the RNG theory, namely,

$$C_\mu = 0.085, \sigma_k = \sigma_\epsilon = 0.7179, C_{1\epsilon} = 1.42, C_{2\epsilon} = 1.68.$$

In the second RNG model two more modifications are included. The turbulent Prandtl numbers are allowed to vary with the local eddy viscosity ν_t via

$$\sigma_k = \sigma_\epsilon = 1/\alpha, \text{ where}$$

$$\left| \frac{\alpha - 1.3929}{0.3929} \right|^{0.6321} \left| \frac{\alpha + 2.3929}{3.3929} \right|^{0.3679} = \frac{\nu}{\nu_t + \nu}.$$

A non-zero R term is also included, where

$$R = \frac{C_\mu \eta^3 (1 - \eta / 4.38) \epsilon^2}{1 + 0.012 \eta^3 k}, \text{ and } \eta = \frac{Sk}{\epsilon}.$$

(for further details see eg. Orszag et al. 1993). The extra features of model R2 are intended to better capture regions of lower turbulent diffusion and high shear. For all three

models, standard equilibrium wall functions were used to model the near wall region.

Inlet Conditions

The experimental data at station 1 was used to derive inlet conditions for the computations. However, not all quantities of interest were measured, so some inlet modelling was unavoidable.

Mean velocities: For the mean velocities at the inlet, we used two methods. In the first method, the inlet distributions of mean axial and swirl velocities were set directly from the experimental profiles. Our second method was to assume a solid-body rotational flow with a uniform axial velocity U_0 . In both cases the radial velocity was set to zero, and both methods have the same inlet flow rate and Swirl number.

There was little difference between the two sets of profiles, as can be seen from the two inlet axial velocity profiles shown in Fig. 2(a). We did not expect that the computations would be noticeably dependent on either choice. In fact, they were, as discussed later.

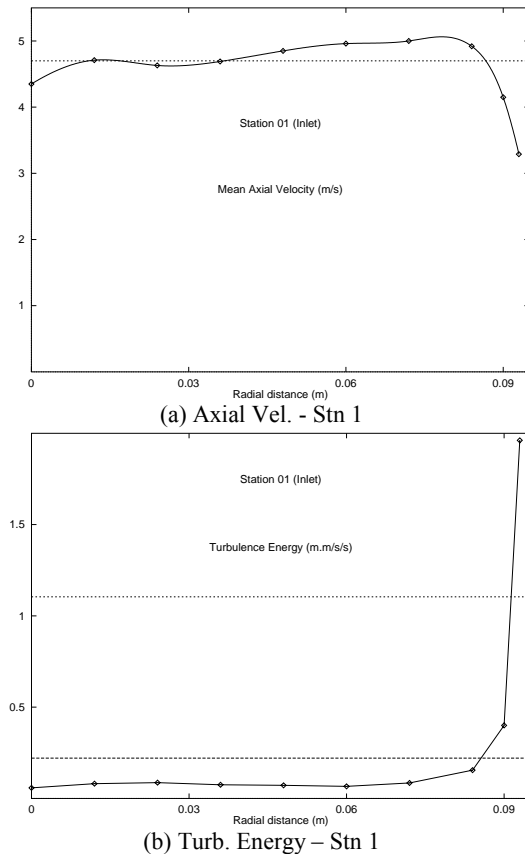


Figure 2: Inlet profiles (a) Axial velocity: IC1 \diamond & IC2 \dashv . (b) Turb. Energy: IC1/IC2 \diamond \dashv , IC3 (Meth. 2, $I=0.01$) \dashv , IC4 (Meth. 2, $I=0.05$) \dots .

Turbulence energy: Modelling of k at the inlet was needed, because only two of the normal stresses were measured. Again, two distinct methods were employed. For the first method, an estimate for k was obtained by first estimating the unmeasured mean square radial velocity as the average of the mean square axial and tangential velocities. The second method estimated k via a turbulence intensity level I and U_0 .

$$\text{Method 1: } k = \frac{u^2 + v^2 + w^2}{2}, \text{ where } v^2 = (u^2 + w^2)/2$$

$$\text{Method 2: } k = IU_0^2$$

Method 1 was used by Benim, whereas Weber et al. used method 2 with $I=0.01$ and 0.05 . The two methods are compared in Fig. 2(b). It can be seen that choosing method 2 with $I=0.01$ overpredicts, by up to 2.5 times, the inlet k profile obtained via method 1 for over 80% of the inlet radius. The inlet levels using $I=0.05$ are even higher.

Dissipation rate: In the absence of measurements, we modelled the inlet dissipation rate via a frequently used relation of the following form.

$$\varepsilon = \delta_\varepsilon \left(\frac{C_\mu^{3/4} k^{3/2}}{0.01 r_i} \right)$$

For comparison purposes, we have included a proportionality factor δ_ε to account for a length scale which needs to be specified, but there is no consensus on its value. Benim used $\delta_\varepsilon=1.00$ (corresponding to about 6% of the inlet radius r_i), Weber et al. used 1.43, while a value of 0.16 has also been used (Hogg & Leschziner 1989, Sharif & Wong 1995). To assess the effect of inlet dissipation rate on the solutions, it seems clear that δ_ε should be treated as a free parameter with a possible range of values over at least one order of magnitude.

Summary of inlet conditions: To gauge the sensitivity of the model to inlet conditions, we tried six different combinations of the alternatives described above, which we aimed to be representative of the many choices reported in the literature. The different inlet conditions are designated IC1 through IC6, and summarised in Table 1.

Table 1: Inlet conditions

Inlet Cond.	Axial Vel.	Swirl Vel.	Turb. Energy	Dissn. (δ_ε)
IC1	Expt.	Expt.	Meth. 1	1.0
IC2	Uniform	S'body	Meth. 1	1.0
IC3	Uniform	S'body	$I=0.01$	1.0
IC4	Uniform	S'body	$I=0.05$	1.0
IC5	Uniform	S'body	$I=0.05$	0.5
IC6	Uniform	S'body	$I=0.05$	0.1

Numerical Method and Grid

To solve the axisymmetric formulation of the Reynolds-averaged Navier-Stokes equations, we used a version of the same finite-volume code Fluent used by Weber et al. in their study. Here the pressure-velocity coupling was resolved using the SIMPLEC procedure (van Doormaal & Raithby, 1984), and results presented below were obtained using the QUICK convective differencing scheme (Leonard, 1977).

Fig. 3(a) shows detail of the *coarsest* grid used here. Note that the spacing is close to uniform in each section. The furnace length was initially set at $L=4\text{m}$, which corresponds to a coarse 217×24 mesh. After extensive trials (see Kelson et al., 1996), it proved possible to move the exit plane upstream without introducing any differences in all relevant quantities. Conservative choices were found to be $L=1.5\text{m}$ for STD model, and $L=2\text{m}$ for models R1 and R2.

For the grid resolution study we used two finer grids, obtained by successively halving the axial grid spacing. For the three grids, Fig. 3(b) shows the computed swirl velocity profile for STD model and IC2 inlet conditions at station 6, using the QUICK scheme. The computed profiles for the two finest grids are virtually coincident. This plot is completely representative of the spatial accuracy achieved for all relevant quantities at all ten stations. In view of this, computations were subsequently performed on the coarser of the two refined grids.

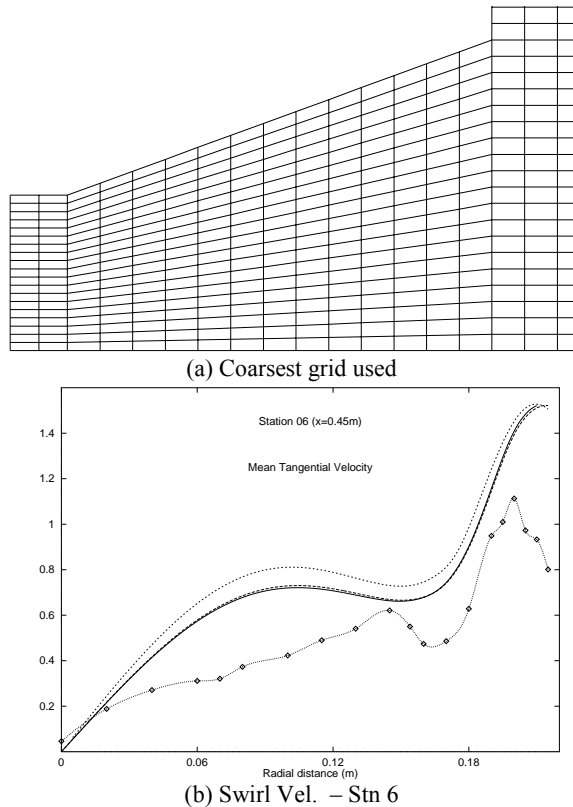


Figure 3: (a) Coarse grid details (b) Std/IC2 profiles at Stn 6: 362x24 (cts), 182x24 --, 92x24 ··· grids. Expt $-\diamond-$.

RESULTS AND DISCUSSION

Measurement stations 4 to 7 cover about two-thirds of the axial extent of the observed IRZ. We will mainly focus on predictions at these stations in the following.

Shown in Fig. 4 are results obtained using Std model for axial and swirl velocity profiles at station 6, along with measurements. Inlet conditions IC1 and IC2 were used, and the predicted profiles, both here and at upstream stations, are significantly different to each other. At this station, the assumption of inlet solid-body rotational flow gives results in better agreement with experiment, but at other stations the predictions obtained using IC1 conditions were superior. Notwithstanding these differences, it is clear from Fig. 4(a) that the extent of axial flow reversal in the IRZ is significantly overpredicted using either inlet condition. Consequently, the two-celled structure was not captured.

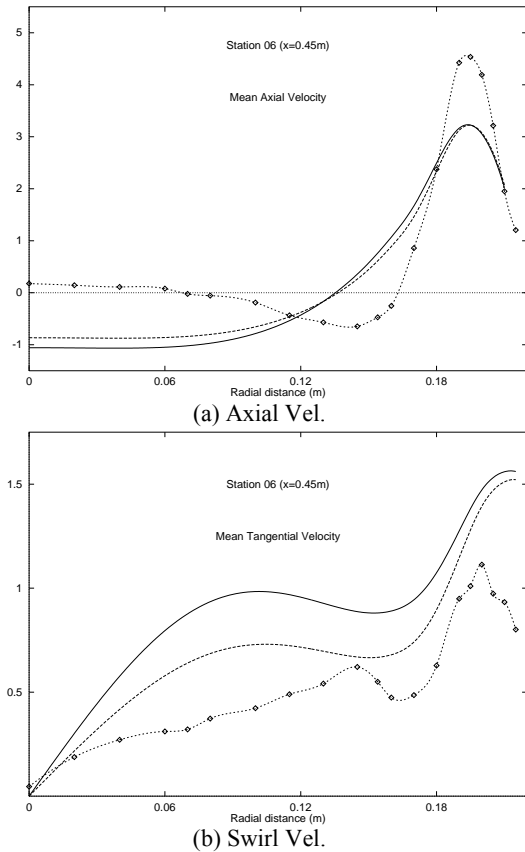


Figure 4: Std/182x24/1.5m model results using IC1 (cts) & IC2 (--) conditions at stn 6 cf. Expt $(-\diamond-)$.

Shown in Fig. 5 are computed profiles of $\sqrt{2k/3}$ at stations 3 and 4 for STD model, using inlet conditions IC2 to IC6. For comparison, the measurements of fluctuating axial and tangential velocities are also shown. Conditions IC2 to IC6 correspond to successively higher turbulence energy levels at Station 3. This is consistent with the corresponding higher inlet turbulence energies and lower inlet dissipation rates used.

Examining the profiles at station 4, we note that the STD model predicts a sharp rise in k just downstream of the breakdown. The rise is clearly too high compared with the measurements. Comparing with the levels shown at station 3, we see that this sharp rise is enhanced if the upstream levels are of a comparable or higher level, as occurs if inlet conditions IC5 or IC6 are used. Relatively higher levels corresponding to conditions IC5 and IC6 were also evident in the profiles at subsequent stations.

Examination of results at all stations revealed that use of conditions IC2 to IC4 did not affect the mean profiles significantly. Use of IC5 and IC6 conditions resulted in noticeable changes, and these were in worse agreement with experiment. We conclude that the inlet turbulence profiles can be important for this flow. If these lead to turbulence levels in the upstream flow which are too high, then levels within the IRZ can be raised, and the predicted mean flow characteristics will be adversely altered.

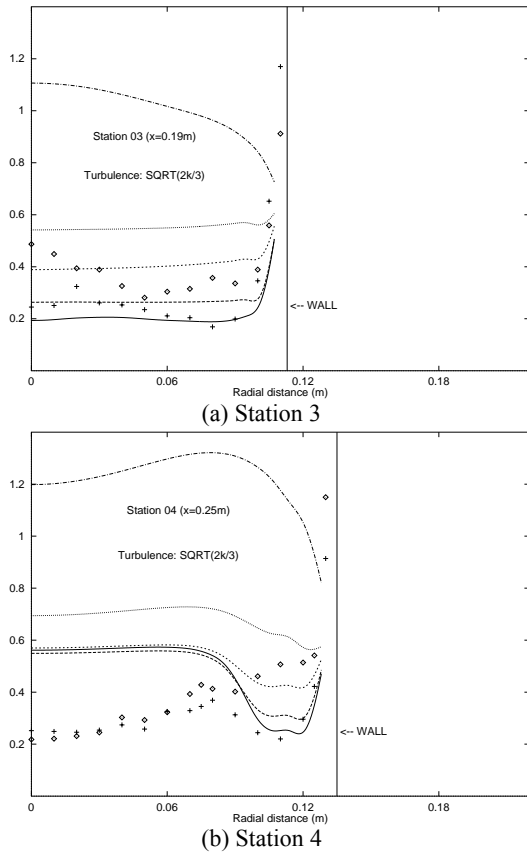


Figure 5: Std model $\sqrt{2k/3}$ profiles at stations 3 & 4 using IC2 (cts), IC3 (long -), IC4 (short -), IC5 (···) & IC6 (-•-) conditions cf. Expt ($u \diamond, w +$).

The STD model results obtained here are not in agreement with experiments. However, a qualitative comparison showed that our results are more favourable than those obtained by either Weber et al. or Benim.

Shown in Fig. 6 are axial velocity profiles for models R1 and R2 for stations 4 to 7. Both models yield clearly superior predictions to the STD model, and closely mimic the experimental data in the IRZ. Model R1 yields the best predictions in the near-axis region, and picks up the two-celled IRZ structure. A qualitative comparison showed that the model R1 profiles are clearly superior to Benim's results using a more complex algebraic stress model. The profiles also appear to be equal or better than the corresponding results of Weber et al. using both algebraic and differential stress models. For example, in Weber et al.'s computations, the two-celled IRZ structure was not quite resolved. Our results suggest that the effects of turbulence anisotropy do not need modelling in order to capture the important flow features.

Shown in Fig. 7 are the mean swirl and turbulence energy profiles at stations 6 and 7. Here again, model R1 closely mimics the observations. Examining the $\sqrt{2k/3}$ profiles shown in Fig. 7(b) suggests that the main reason model R1 yields better mean flow predictions is that the computed turbulence levels within the IRZ seem more consistent with the measurements.

Although not given here, plots of the centreline eddy viscosity showed that, overall, model R1 predicts a more gradual rise in eddy viscosity just inside the IRZ. To investigate why this was so, we performed separate

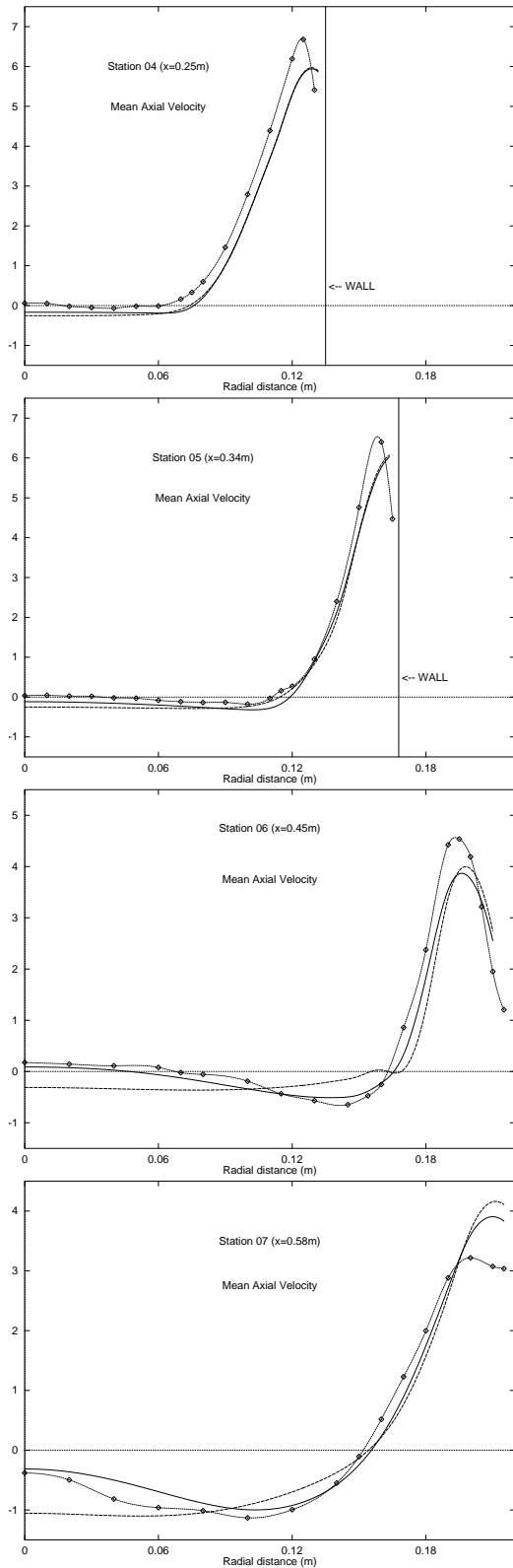
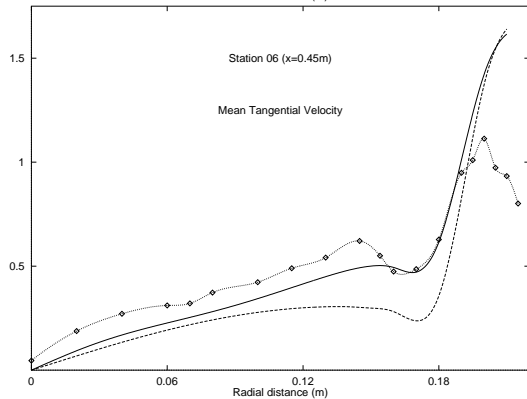
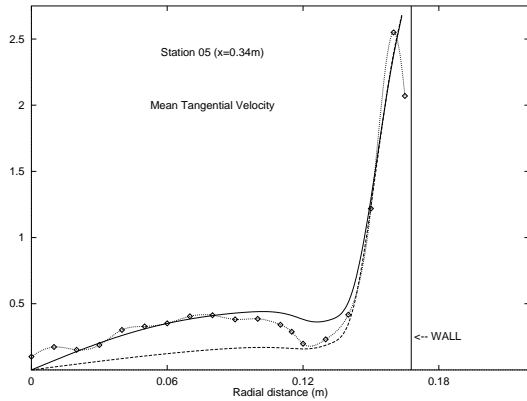
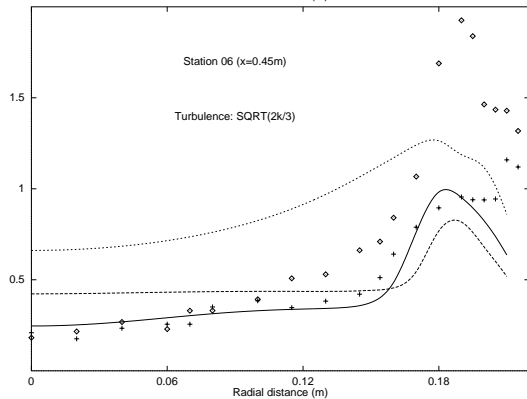
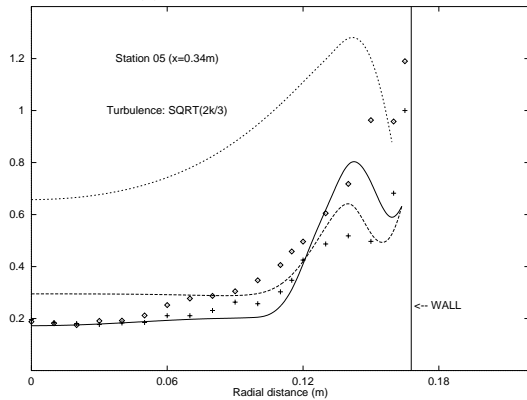


Figure 6: Comparison of 232x24/2m mean axial vel. profiles at stations 4, 5, 6 & 7 for models R1 (cts) and R2 (-) using IC1 conditions, with Expt ($-\diamond-$).

computations with models where only a single constant in STD model was altered to its model R1 value. It was clear that changing the constant $C_{2\varepsilon}$ in the dissipation rate equation had the most dramatic effect in reducing



(a) Swirl vel. – Stns 5 & 6



(b) $\sqrt{2k/3}$ - Stns 5 & 6

Figure 7: Comparison of 232x24/2m/IC1 profiles at stations 5 & 6. (a) Swirl vel. for models R1 (cts) & R2 (--) cf. Expt ($-\diamond-$); (b) $\sqrt{2k/3}$ for models R1 (cts), R2 (--) & Std (\dots) cf. Expt ($u \diamond, w +$).

centerline eddy viscosity levels of the STD model. Changing only the turbulent Prandtl numbers σ_k and σ_ϵ had a lesser effect, while changing constant $C_{1\epsilon}$ resulted in a very slight increase.

CONCLUSIONS

A computational study of flow in a quarl burner has been reported here, using three two-equation turbulence models. A number of points have been made, and we summarize the main ones below.

1. We show that two sets of inlet mean profiles IC1 and IC2, which correspond to the same inlet flow rate and Swirl number, are nevertheless *not* equivalent. The relatively small differences involved lead to significant differences in the computations, and must be accounted for in the turbulence model assessment.
2. For this flow, the inlet turbulence profiles can also be important. If these lead to turbulence levels in the upstream flow which are too high, then levels within the IRZ can be raised, and the predicted mean flow characteristics will be altered.
3. Results for the STD model do not agree with experiment, but its performance is not as bad as previous studies of this flow have suggested.
4. With respect to the flow physics, we argue that the structure of the IRZ is mainly governed by turbulence levels within it. The STD model fails because it overpredicts turbulence levels within the recirculating zone. However, a STD model with modified constants predicted by RNG theory returns lower levels in the IRZ, and captures the complex two-celled structure. The improvement is largely due to changing the constant $C_{2\epsilon}$ in the dissipation rate transport equation, highlighting the problematic role this equation plays in turbulence modelling at this level of closure.

Acknowledgements

Financial support for this work was funded in part by BHP research. Computing facilities were supplied by Digital under agreement DEC ERP No. 2057.

REFERENCES

- BENIM, A. C. (1990), "Finite element analysis of confined turbulent swirling flows", *Int. J. Num. Meth. Fluids*, **11**, 697-717.
- HAGIWARA, A., BORZ, S., and WEBER, R. (1986), "Theoretical and experimental studies on isothermal expanding swirling flows with application to swirl burner design - results of the NFA 2-1 investigations", Technical Report Doc. F 259/a/3, International Flame Research Foundation.
- HALL, M. G. (1966), "The structure of concentrated vortex cores", *Prog. Aeronautical Sci.*, **7**, 53-110.
- HOGG, S., and LESCHZINER, M. A. (1989) "Computation of highly swirling confined flow with a Reynolds-stress turbulence model", *AIAA J.*, **27**, 57-63.
- KELSON, N. A., McElwain, D. L. S., and TRUELOVE, J. S. (1996), "Computation of turbulent flow in an IFRF quarl burner", Technical report, Queensland University of Technology CiSSaIM Tech. Rpt. 96/5.
- LEONARD, B. P. (1977), "A stable and accurate convective modelling procedure based on quadratic upstream interpolation", *Computer Meth. Appl. Mech. and Eng.*, **19**, 59-98.

ORSZAG, S. A., YAKHOT, V., FLANNERY, W. S., BOYSAN, F., CHOUDHURY, D., MARUSZEWSKI, J., and PATEL, B. (1993), "Renormalization group modeling and turbulence simulations". In R. M. C. So, C. G. Speziale, and B. E. Launder, editors, *Near-Wall Turbulent Flows*, pp 1031-1046. Elsevier.

SHARIF, M. A. R. and WONG, Y. K. E. (1995), "Evaluation of the performance of three turbulence closure models in the prediction of confined swirling flows", *Computers and Fluids*, **24**, 81-100.

SMITH, L. M. and WOODRUFF, S. L. (1998), "Renormalization-group analysis of turbulence", *Annu. Rev. Fluid Mech.*, **30**, 275-310.

VAN DOORMAAL, J. P. and RAITHBY, G. D. (1984), "Enhancements of the SIMPLE method for predicting incompressible fluid flow", *Numer. Heat Transfer*, **7**, 147-163.

WANIK, A. and SCHNELL, U. (1989), "Some remarks on the PISO and SIMPLE algorithms for steady turbulent flow problems", *Computers and Fluids*, **17**, 555-570.

WEBER, R., VISSER, B. M. and BOYSAN, F. (1990), "Assessment of turbulence modeling for engineering prediction of swirling vortices in the near burner zone", *Int. J. Heat and Fluid Flow*, **11**, 225-235.